

### Flow Separation Noise Sources

Alexandre Suryadi<sup>a</sup>, Michaela Herr

Institute of Aerodynamics and Flow Technology, German Aerospace Center (DLR), Germany

<sup>a</sup> Corresponding author: Lilienthalpl. 7, 38108 Braunschweig; alexandre.suryadi@dlr.de

The DLR Impulse project SAFER<sup>2</sup> aims to develop a machine learning model for the detection of turbulent boundary layer separation induced by an adverse pressure gradient. Whereas identifying turbulent separation itself remains a challenging topic, it is also necessary to classify the noise penalty to the degree of flow separation. This paper investigates the flow separation noise of a 2.1 m span NACA 64-618 wing model installed in the 3/4-open anechoic test section of the Low-Speed Wind Tunnel Braunschweig (NWB) of the German-Dutch Wind Tunnel (DNW), figure 1a. The same figure shows the phased microphone array with 140 LinearX M51 1/2" microphones and 10, 1/2" Bruel&Kjær free-field microphones were distributed equally facing each side of the blade model as sketched in figure 1b. Aerodynamic parameters were measured using a load balance installed under the floor of the test section and, additionally, 5 spanwise distributed static pressure taps, totaling 281, monitor the model's pressure distribution. Three boundary layer states were measured (1) naturally transitioning (*Clean*) and forced transition (*Trip*) with 0.4 mm high zig-zag tapes at two positions: (2) at 5% local chord length ( $c$ ) on the suction side (SS) and 10% $c$  pressure side (PS), and (3) at 25% $c$  SS and 10% $c$  PS. Aerodynamic forces and far-field noise were measured at wind tunnel speeds of  $U_0 = 44, 52, 60, 70, 80$  m/s and at 12 angles-of-attack from  $\alpha = 0^\circ, 2^\circ, 4^\circ, 5.5^\circ, 9^\circ, 10^\circ, 13^\circ, 16^\circ, 18^\circ, 20^\circ, 21^\circ, 23^\circ$ . Note that  $\alpha$  corresponds to the geometric angle of attack, and no angle correction is made here.

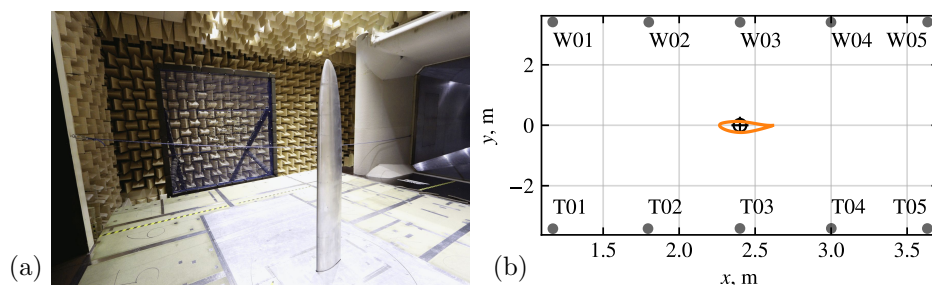


Figure 1: (a) Experimental setup in the NWB and (b) a sketch of the free-field microphone positions: (W01...5; T01...5) around the model. The flow is from left to right.

Analysis of the far-field noise using the coherent output power (COP) method [1] produces a large coherence,  $\gamma$ , and a phase angle,  $\theta$ , around  $\pi$  within a frequency range that characterizes trailing-edge noise as shown in figure 2. It follows from the coherence identity that the measured far-field noise spectrum can be discriminated into its coherent, i.e. COP, and incoherent parts in figure 3a. With increasing  $\alpha$ , the coherent part has a maximum that shifts to a lower frequency, whereas the incoherent part has increasing relevance at higher frequency. Their scaling with the Mach number,  $Ma$ , is shown in figure 3b. The coherent part scales according to  $Ma^{\approx 5}$  of an edge radiated noise [2] and the incoherent part scales with  $Ma^{>5}$  from  $\alpha \geq 9^\circ$ . Sound localization with the phased microphone array shows that the incoherent part consists of the tip noise at a high frequency and noise at an intermediate frequency that seems to be detached from the edge. These sound maps are shown in figure 4.

The present result shows that the elements of flow separation noise consist of a low-frequency edge-radiated noise that can be modeled using a turbulent wall-pressure model [3] and a mid-frequency noise that is, seemingly, detached from the edge. So far, the modeling of the latter is not fully understood. The full paper will present the methodology, aerodynamic results, and noise source localization.

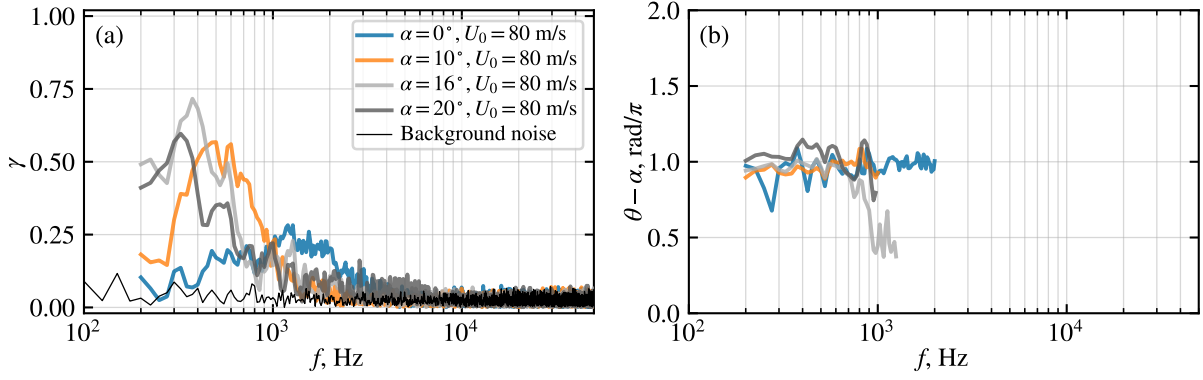


Figure 2: (a) Coherence spectra and (b) phase angle spectra of 4  $\alpha$ s (*Trip* 05/10) and the background noise of the wind tunnel.

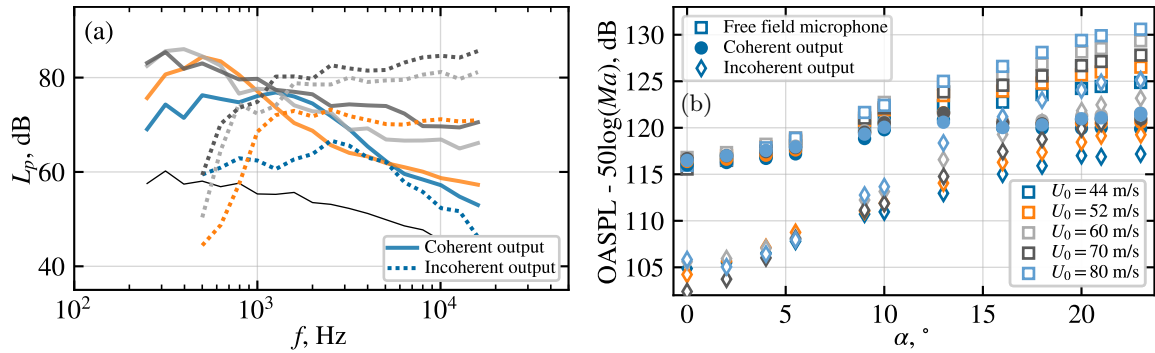


Figure 3: (a) One-third octave band spectra, the line color follows the legend in figure 2a and (b) OASPL vs  $\alpha$ .

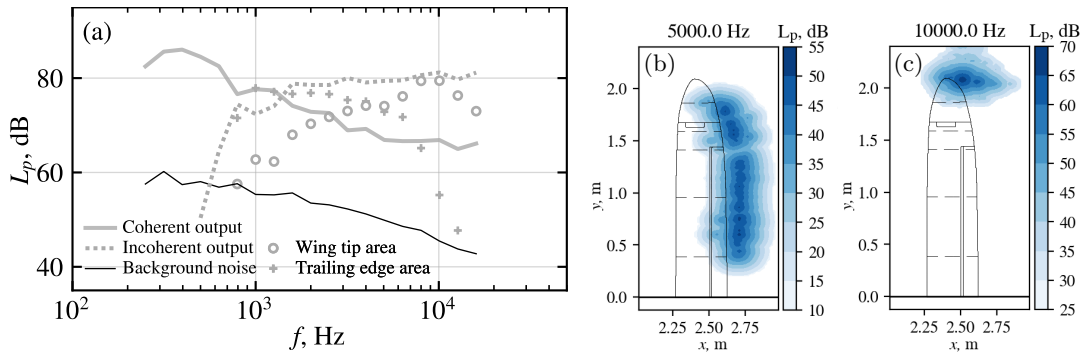


Figure 4: Noise source maps of the NACA 64-618 wing model,  $\alpha = 16^\circ$  and  $U_0 = 80 \text{ m/s}$ : (a) breakdown of the noise spectrum, (b) around the trailing edge and (c) around the tip at a selected frequency.

## References

- [1] Florence V. Hutcheson and Thomas F. Brooks. Measurement of Trailing Edge Noise Using Directional Array and Coherent Output Power Methods. *International Journal of Aeroacoustics*, 1(4):329–353, 2002.
- [2] J. E. Ffowcs Williams and L. H. Hall. Aerodynamic sound generation by turbulent flow in the vicinity of a scattering half plane. *Journal of Fluid Mechanics*, 40(04):657, 1970.
- [3] Alexandre Suryadi. Prediction of Trailing-Edge Noise for Separated Turbulent Boundary Layers. In A. Dillmann, G. Heller, E. Krämer, C. Wagner, C. Tropea, and S. Jakirlić, editors, *New Results in Numerical and Experimental Fluid Mechanics XII*, volume 142 of *Notes on Numerical Fluid Mechanics and Multidisciplinary Design*, pages 769–779. Springer, Cham, 2018.